Environment International 127 (2019) 573–583

Contents lists available at ScienceDirect

Environment International

journal homepage: www.elsevier.com/locate/envint

Exploring the mechanisms of heat wave vulnerability at the urban scale based on the application of big data and artificial societies

Cheng He[a,c,d], Liang Ma[b], Liguo Zhou[a,c], HaiDong Kan[e], Yan Zhang[a,c,d], WeiChun Ma[a,c,d,*], Bin Chen[b,**]

[a] Department of Environment Science and Engineering, Fudan University, Shanghai 200082, China
[b] College of System Engineering, National University of Defense Technology, Changsha 410073, China
[c] Big Data Institute for Carbon Emission and Environmental Pollution, Fudan University, China
[d] Shanghai Institute of Eco-Chongming (SIEC), No. 3663 Northern Zhongshan Road, Shanghai 200062, China
[e] School of Public Health, Fudan University, Shanghai 200032, China

ARTICLE INFO

Editor: Yong-Guan Zhu

ABSTRACT

Rapid urbanisation has altered the vulnerability of urban areas to heat wave disasters. There is an urgent need to identify the factors underlying the effect of heat waves on human health and the areas that are most vulnerable to heat waves. In this study, we plan to integrate indices associated with heat wave vulnerability based on meteorological observation data, remote sensing data and point of interest (POI) data; analyse the influence of urbanisation on the urban vulnerability environment; and explore the relationship between the vulnerability environment and heat-wave-related mortality. Finally, we attempt to map the spatial distribution of high heat-wave-related mortality risk based on the results of heat wave vulnerability study and artificial society. The results reveal that 1) there are differences in the influence of urbanisation on heat wave exposure, sensitivity and adaptability; 2) the exposure and sensitivity level effects on the lower limit of health impacts and the adaptability level effects on the upper limit of the health impact from heat wave in a given study area; and 3) areas vulnerable to the effects of heat waves are not confined to the city centre, which implies that residents living in suburban areas are also vulnerable to heat waves. Finally, this study not only explores the factors contributing to the impacts of heat waves but also describes the spatial distribution of the risk of disaster-associated mortality, thereby providing direct scientific guidance that can be used by cities to address heat wave disasters in the future.

1. Introduction

Heat wave disasters, an extreme weather event result from climate change impact, has seriously affected human society (Marsha et al., 2018; Reid et al., 2009). Recent studies have confirmed that excessive heat affects lung functions and blood flow in the human body and has a direct impact on cardiovascular disease (Braga et al., 2002; Curriero et al., 2002). Furthermore, many studies have demonstrated the relationship between heat waves and population mortality (Anderson et al., 2016; Chien et al., 2016). Specifically, > 7000 people died during the 2003 European heat wave event (Della-Marta et al., 2007; Fouillet et al., 2006), and > 50,000 people died during the 2010 Russian heat wave disaster (Hauser et al., 2016). In urban areas, the risk level is even higher. Recently, the intensity, frequency and duration of extreme hot weather events have increased in cities around the world (IPCC, 2007), and this increase may lead to dramatic increases in heat-related mortality and influence the development of the urban social environment. For example, during the 2010 heat wave event in Xi'an, China, the ratio of high-temperature mortality was 30% higher than that in other periods (Huang et al., 2010).

Urban areas are recognisably more vulnerable to high temperatures due to the “urban heat island” effect (Fallmann et al., 2016; Giannaros et al., 2013). Heat wave impacts within urban areas, however, are determined not only by disaster exposure but also by a city's sensitivity and adaptive capacity according to the IPCC (IPCC, 2014). Specifically, suburban areas with high sensitivity and a limited adaptive capacity are especially vulnerable to heat waves. Therefore, the influence of urbanisation on urban vulnerability may be synthesised and classified

* Correspondence to: W. Ma, Department of Environment Science and Engineering, Fudan University, Shanghai 200082, China.
** Corresponding author.
E-mail addresses: wcma@fudan.edu.cn (W. Ma), nudtcb9372@gmail.com (B. Chen).

https://doi.org/10.1016/j.envint.2019.01.057
Received 16 August 2018; Received in revised form 22 January 2019; Accepted 22 January 2019
Available online 12 April 2019

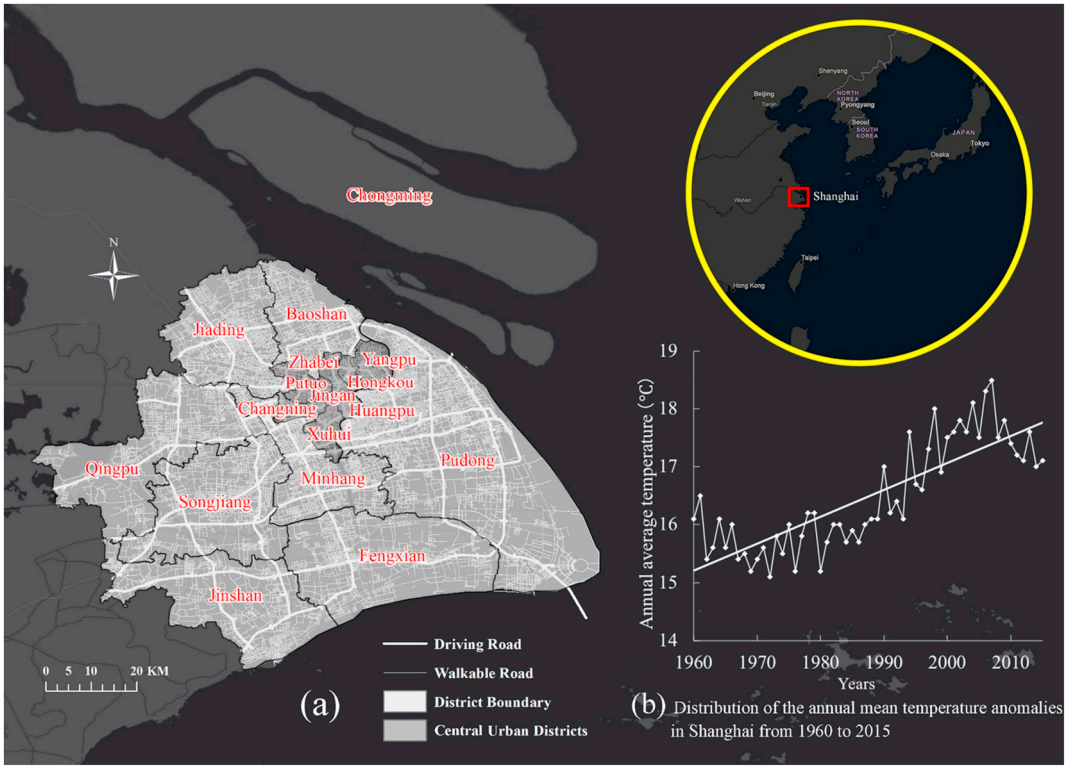

Fig. 1. Distribution area of Shanghai. (a) Spatial distribution of each district in Shanghai, including the various road types of roads in the city. According to the analysis conducted in this article, roads are divided into two categories: driving roads (urban expressways and freeways) and walkable roads (national roads, provincial roads, county roads and pedestrian roads in cities). (b) Annual mean temperature from 1960 to 2015. The straight white line depicts the linear regression of the mean temperature data from different years.

(Alana et al., 2008). To be specific, the exposure level and sensitivity factors increase along with the urbanisation process, although high temperature adaptability is also enhanced, because of the increasing social awareness and economic level of residents.

Few studies have examined the relationship between the three different change aspects of vulnerability to human health, although many studies have examined vulnerability indices according to vulnerability features. In terms of exposure, early studies primarily developed indices based on air temperature observation data (Aubrecht and Ozceylan, 2013; Basu, 2009; Hajat et al., 2010). These data can be used to explain the temperature change for long time series within a specific area. To depict the temperature distribution pattern more precisely, recent research has used satellite-derived estimates of land surface temperature (LST) (Hondula et al., 2015), with the MOD11A1 LST being utilised in most studies (Westermann et al., 2011; Zheng et al., 2014). Produced by the MODIS Science Team, the MOD11A1 LST is a daily 1-km product. However, exposure to high temperatures is characterised not only by variable temperature but also by the duration and frequency of heat waves (Mazdiyasni et al., 2017). Thus, the spatial distribution and changes in temperature in time series should be considered in exposure evaluations. In terms of sensitivity, the more sensitive groups are the elderly and children (Cutter and Finch, 2008; Diaz et al., 2015) and those who live below the poverty line (Reid et al., 2009) or in isolated social conditions (Johnson et al., 2012). Other sensitivity indicators include race, educational background and social status (Reid et al., 2009; Semenza et al., 1996; Uejio et al., 2011). However, these indicators are restricted by the statistical scale. Especially in China, the unit area of this statistical data is too large to evaluate within a single urban area. In terms of adaptability, past studies have evaluated various adaptive indicators, such as the use of air conditioning, the condition of the cooling infrastructure and the availability of medical resources (Johnson et al., 2012; Westermann et al., 2011). At the city scale, however, information about these indices is also limited for quantification at a higher spatial resolution.

Recent studies have constructed large-scale simulation systems to address complex problems based on the development of computer simulation algorithms (Epstein, 2009), which provide a new quantitative study method for complex social problems (Helbing, 2013; Wu and Birkin, 2012), especially in the field of public health management. Typical examples of this research include studies on how disease spreads in an urban social network by modelling complex social behaviour (Epstein, 2009) and simulating the impact of public policies (Wu and Birkin, 2012) or economic development (Jordan et al., 2012) in complex processes. This method has often been used in epidemiological research and is very suitable for studying urban environmental problems; however, it has been minimally used for heat wave disaster studies. On the other hand, with the rapid development of big data, new spatial geographic data are used to represent social and economic activities, such as using urban night-time light (NTL) and Google's point of interest (POI) data to identify urban centres (Cai et al., 2017), researching urban spatial expansion through check-in data from social media (Zhen et al., 2017) and using electronic map data to identify urban residents' activity areas (Puliafito et al., 2015). Therefore, these new methods and data sources may be used to solve the index selection problems and describe heat wave vulnerability in urban areas in a more comprehensive and accurate manner.

Based on the present situation, this research aims to 1) quantitatively evaluate heat wave vulnerability indices through the use of multitype geospatial data, such as network POI data, road spatial data, NTL data and remote sensing data; 2) depict the distribution characteristics of each index by quantifying the influence of urbanisation on the urban vulnerability environment and analyse which type of influence has an obvious impact on human health under different heat wave conditions using a logistic regression model; and 3) identify the specific distribution of high heat-wave-mortality risk based on the vulnerability environment and an artificial society to obtain the distribution of heat-

wave-related mortality risk in the study area. Ultimately, this study proposes to answer the following key questions: 1) How does urbanisation influence the heat wave vulnerability in an urban area? 2) Compared with different degrees of heat-related mortality, what factors affect human health under the conditions presented by heat waves? 3) How are high heat-related mortality risk areas distributed, and what are the relationships between these areas and sensitive populations? The responses to these questions will influence urban planning and advice for the increasingly severe heat wave disasters in Shanghai.

2. Study area

Shanghai is the economic centre of China, with 24.20 million people distributed across 6340.50 km^2 of land (from Shanghai Statistics Bureau, http://www.stats-sh.gov.cn/). Shanghai is the largest city on the southeast coast of China, and it is located at the mouth of the Yangtze River (Fig. 1a). In summer, the subtropical high-pressure zone always leads to unbearably hot weather in this area. Apart from that, the permanent population in Shanghai growing at a high speed since the development of Pudong in 1990, it increased by 75.35% from 2000 to 2010 (Han et al., 2018). The spatial structure and natural environment within the city have experienced considerable changes, and temperatures have increased as shown in Fig. 1b. At 14:00 on 21 July 2017, the temperature observed at Xujiahui station in Shanghai reached 40.9 °C, breaking the previous high temperature record and resulting in severe impacts on the urban environment. These phenomena are the primary motivation for our research.

Because natural conditions and social activity characteristics are considered simultaneously in the study, we only included the traditional area of Shanghai (excluding Chongming Island) as the research area, because Chongming is predominantly a natural environment and the comprehensive evaluation factors are not suitable to describe this area.

To unify the resolution of various evaluation data and facilitate a unified analysis, the spatial distribution of a 500 * 500-metre grid that included all districts in the study area was generated using the ArcGIS fishnet tool as the statistical basis for this study.

3. Definition of heat wave

The concept of a heat wave refers to instances in which certain stresses on natural and societal systems occur when the temperature exceeds a certain threshold (Anderson and Bell, 2009). Generally, a heat wave occurs when the temperature exceeds a certain threshold on a given number of consecutive days (Tan et al., 2007). Therefore, a complete definition of a heat wave involves two main variables: 1) a high temperature threshold and 2) the number of consecutive days over which the temperature exceeds the threshold. The two values will vary for different locations depending on the varying influences of temperature (Keellings and Waylen, 2014). Based on the above two variables, the definition of a heat wave used in this study is as follows: (1) Temperature threshold: This study defines a heat wave event as the T_{max} (highest temperature) and T_{min} (lowest temperature) for a given day that are > 90% of the values for other days of the year. Combining the T_{max} and T_{min} to define the heat wave events aims to eliminate the phenomenon of cooling that occurs at night. (2) Number of continuous days: If the interval between heat wave events is less than three days, then the events are considered one single event; otherwise, the events are considered multiple, independent events. This method considers the influence of the overlap between epidemiological events, and it is also consistent with results that there is a weak link between heat-wave-related deaths measured every day and those measured every three days (Curriero et al., 2002).

Fig. 2 shows the process of defining the heat wave events used in this study. Although the highest temperature exceeded the threshold on both 27 and 28 August, the lowest temperature did not exceed the threshold on those days; therefore, those days were not included in the heat wave event. In E2, from 15 to 18 August, the requirement of exceeding both the T_{max} and T_{min} threshold was not met. While, based on the standard of judging independent events for 3 days, this heat wave was regarded as a single event occurring from 13 to 20 August.

4. Data and methodology

4.1. Data sources for HVI

To estimate the risk of heat-related health impacts, many studies have developed heat vulnerability indices (HVIs) using a combination of exposure, sensitivity and adaptability indices based on a vulnerability definition (IPCC, 2014). Exposure can be understood as the proximity of people or systems to disasters (Fussel, 2007; Kelly and Change, 2000; Turner et al., 2012). Sensitivity is characterised by the maximum impact from a disaster that a system can bear (Díaz et al., 2018; Fussel, 2007). Different system areas are able to tolerate different maximum impacts from heat wave disasters due to their varying qualities (Curriero et al., 2002). Adaptability refers to the ability of a system or person to change their own state and behaviour in an effort to better adapt to existing or expected pressure from a disaster (Cutter and Finch, 2008).

Accordingly, we have selected seven variables that are relevant to the three HVI components.

4.1.1. Spatial variables for heat wave exposure

The degree of exposure will differ depending on the physical attributes of the disaster event (Ho et al., 2017). In this study, we attempt to examine the changes in physical attributes of a heat wave as exposure factors. According to relevant studies, three physical variables are selected across the study area:

(1) Heat wave duration (HWD) refers to the number of days corresponding to the longest heat wave event during the study year. According to Mazdiyasni, the number of deaths associated with heat waves is related to the duration of the longest heat wave during a given year (Mazdiyasni et al., 2017).
(2) Heat wave frequency (HWF) describes the number of heat wave events occurring in a given year. Previous case studies (Aubrecht and Ozceylan, 2013; Mazdiyasni et al., 2017) demonstrate that the number of deaths associated with heat waves is related to the HWF throughout an entire year.
(3) Heat wave intensity (HWI) is expressed as the temperature required to ensure higher exposure with a higher temperature level during a heat wave event. Human activities typically result in built-up environments containing many types of impervious surfaces characterised by a subsequently higher thermal environment distinction inside the city (Johnson et al., 2012). Temperatures in the city centre are significantly higher than those in the surrounding suburbs. Consequently, the impact of temperature on the human body is more prominent in the city centre than it is in the suburbs.

HWD and HWF are obtained from meteorological observation data. First, daily distribution rasters of T_{max} and T_{min} are depicted using the interpolated method of universal kriging based on meteorological data (Hudson and Wackernagel, 2010). Second, the dates for each day's T_{max} and T_{min} were converted into polygon data using ArcPy (batch calculation API of ArcGIS). Third, these polygon dates were matched to the same 500-metre grid such that each grid ID would contain the values of T_{max} and T_{min} for each day at the same time. Then, grid-based "HWD" and "HWF" maps were derived from the heat wave definition, using the batch calculation packages of NumPy and Pandas in Python.

HWI is described using LST. Based on Landsat 8 images, the spatial distribution of the LST is calculated using the LST inversion algorithm (Coll et al., 2010). The acquisition time of Landsat 8 data is 3 August

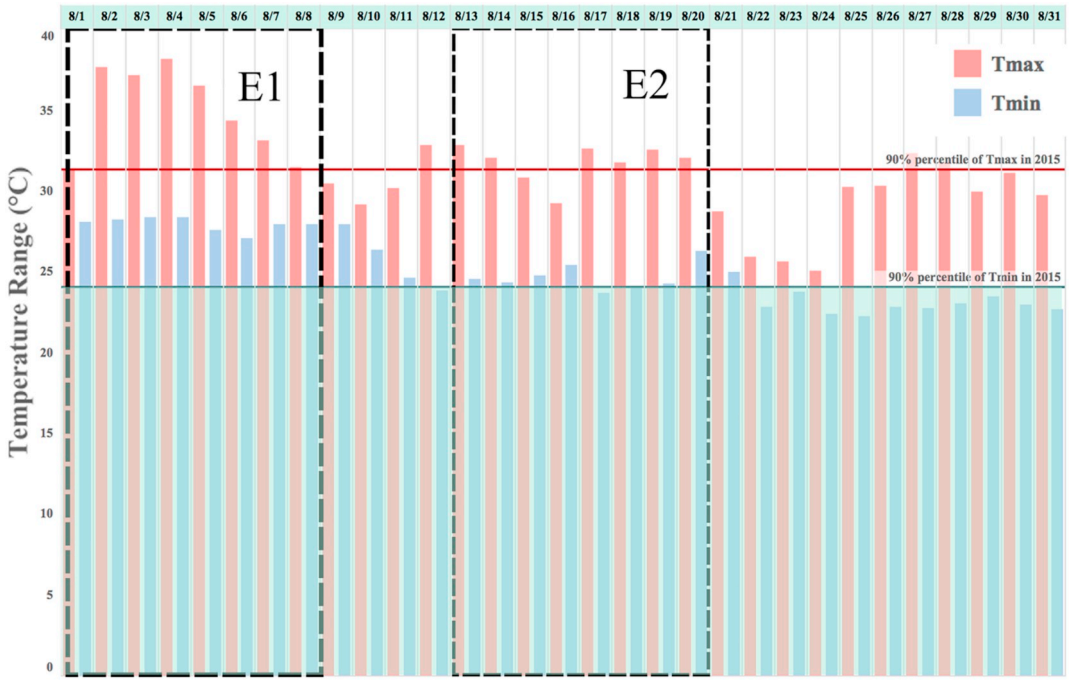

Fig. 2. Observation data from the Minhang Meteorological Observatory for August 2015. All meteorological data used in this paper were obtained from the China Meteorological Data Network (http://data.cma.cn).

2015, when the heat wave incident was observed at all 8 sites across the study area. The Landsat 8 data used in this study were provided by the Geospatial Data Cloud site (http://www.gscloud.cn).

4.1.2. Spatial variables for heat wave sensitivity

Many different indices can be used to express environmental sensitivity within an urban area, and these indices often include many aspects of the urban environment (Chuang and Gober, 2015; Ho et al., 2017; Krstic et al., 2017). We included two indices that have independent relationship with heat wave sensitivity:

(1) Density of roads. In densely populated areas, intensive traffic is an important source of anthropogenic heat emissions (Chow et al., 2014). Areas with highly dense road networks may be more sensitive due to the combination of vehicle exhaust emissions and high air temperatures (Sun et al., 2018). These factors have been used to develop an important vulnerability index in related studies (Krstic et al., 2017). In the present study, the road networks with higher traffic volume, including urban expressways, highways, viaducts and national roads, were obtained using OpenStreetMap (OSM, www.openstreetmap.org), We calculated the length of the selected roads in each 500-m grid section.
(2) Vegetation coverage. High vegetation coverage may regulate the high temperatures through heat absorption; therefore, high vegetation coverage is often associated with a reduction in heat-related mortality. In fact, a study comparing two heat waves in Shanghai in 1998 and 2003 showed that the primary cause of a decrease in mortality was an increase in vegetation coverage at the urban level (Huang et al., 2010). To describe the level of vegetation coverage within the study area, we attempt to represent the vegetation coverage using Li's inversion algorithm based on Landsat 8 data (Li et al., 2014).

4.1.3. Spatial variables for heat wave adaptability

Many different indices can be used to express the adaptability level of people and systems when a heat wave event occurs. We included two indices from relevant research for people and systems.

(1) Availability of medical resources. As important social resources for combating disease, comprehensive hospitals and community health institutes play a key role in maintaining residents' health (Cutter and Finch, 2008). To describe the availability of medical resources in the study area, the specific distribution of all medical sites in Shanghai was obtained using the GAODE map's application programming interface (API). Many studies have used these API data to describe social resources in large cities (Liu et al., 2017; Zheng et al., 2018). The data used in this study were acquired in December 2015. Several medical resources that are relevant to the treatment and prevention of heat-related diseases were selected (including general hospitals, community health centres, clinics and hospitals for the treatment of infectious diseases). In addition, we obtained the spatial distribution of walkable roads in Shanghai using OSM (Fig. 1) to quantify the service scope of these units. Based on the relevant research, the normal walking speed in these walkable areas was assumed to be 4.5 km/h (Andriacchi et al., 1977). The spaces without a distribution of walkable roads were considered to be buildings or other surfaces, in which the normal walking speed was assumed to be 4 km/h. The cost of walking time to the nearest medical sites, which was calculated using the cumulative cost distance tool in ArcGIS, was used to express the availability of medical resources in the study area.
(2) Night-time light (NTL) value. There is a strong association between the socio-economic conditions and the incidence of heat-related diseases in urban areas (Reid et al., 2009). Many studies have attempted to describe the socio-economic conditions using NTL data (Zhang and Seto, 2011) to explain the positive correlation between NTL and the socio-economic conditions in urban areas (Cai et al., 2017). In this study, the annual composites of NTL data from the Visible Infrared Imaging Radiometer Suite (VIIRS) throughout the study years (2015) were collected from the National Centers for Environmental Informational (https://www.ngdc.noaa.gov). The annual composited data are based on day/night band (DNB) data that are filtered to exclude information impacted by stray light, lightning, lunar illumination and cloud cover according to the data description (https://www.ngdc.noaa.gov/eog/viirs/download_dnb_composites.html). To verify the representation of this data, we

calculated the average intensity of the NTL values in each district and performed a linear regression analysis between the NTL values and the per capita GDP for each district in 2015. The results, which had an R^2 of 0.75 and $p < 0.0001$, revealed that the NTL data adequately represent the social and economic spatial distribution within the city.

4.2. Analysis methods for HVI

4.2.1. Factor analysis method for HVI

Many studies have correlated urban areas with high temperatures, where dense populations are at risk and social vulnerabilities are spatially variable (Madrigano et al., 2015a; Reid et al., 2009). It is necessary to classify the urban environment by combining various vulnerability factors to explore the impact of an urban-integrated vulnerable environment on human health.

However, different aspects of urbanisation have a varying influence on urban vulnerability. On the one hand, the level of exposure and sensitivity factors may have increased as the human activity intensity increased during the process of urbanisation. On the other hand, the level of high temperature adaptability may simultaneously be enhanced because of increases in the social and economic levels. In other words, it is possible to separate the integrated vulnerable environment from the influence of urbanisation.

For the integrated approach, unscientific descriptions may be generated when the indices are simply added. Therefore, we chose to classify the vulnerability environment according to the spatial characteristics of the urban environment.

To find more independent aggregated patterns, the varimax rotation method is applied to these selected HVI indices (Wood et al., 1996). The varimax rotation can further simplify the spatial patterns via similarities and maximise the spatial patterns based on their differences. Many studies have used this method to guide the study of vulnerability environments (Chuang and Gober, 2015; Reid et al., 2009). In those studies, each spatial index is assigned a weighted score from the varimax rotation result, and the sum of the weighted indices are aggregated to describe a type of vulnerability environment.

4.2.2. Health impact analysis of HVI

Different types of vulnerability environments can impact health to varying degrees (Reid et al., 2009). To understand how accurately the vulnerability environment reflects actual mortality at the local level, we evaluated the locations and types of urban environments that are at risk of heat-related mortality caused by different types of vulnerability environments beyond social and natural contexts using a multinomial logistic regression model (MLR), which included factor scores from the vulnerability classification as independent variables and daily mortality for heat wave days as a three-category dependent variable (zero, moderate and high mortality). *P*-values and odds ratios (ORs) (95% confidence interval (CI)) were presented for each category, comparing net moderate and high against zero mortality net.

Daily mortality data for the entire year of 2015 were collected from the Pudong Centre for Disease Control. The following information was available for each death: date of death; education level; age; sex; addresses; and cause of death (coded based on the 10th revision of the International Classification of Diseases). A total of 21,858 non-accidental deaths occurred in 2015. To focus on heat-related mortality, we identified 1456 residents who died during the heat wave period according to the definition of heat wave in this study, and the risk ratio (RR) was 1.32 > 1, which explains the contributing impact of high temperatures to these deaths. Then, these deaths were geocoded (including longitude and latitude) using the address interpretation tool of the GAODE map based on the residents' addresses in the database.

We selected Pudong as a research object for the analysis for two reasons. First, the area of Pudong is 1210.41 km^2, which is more than one-quarter of the total area of Shanghai. The differences in the socio-economic and natural conditions in Pudong are evident. The urbanisation level in the north is higher, and it includes Shanghai's financial centre, Lujiazui Street. In the south, the urbanisation level normalises and is characterised in part by an agricultural economy. Second, the level depends on the sea, and the temperature conditions in the region are unstable and easily affected by heat waves in summer.

4.2.3. Method of mapping the mortality risk distribution

The final step was to map the spatial distribution of the high mortality risk areas by comparing the distribution of high heat-wave-related mortality risk and specific sensitive populations.

(1) Distribution of high heat-wave-related mortality risk

Based on the identification of mortality-related vulnerability environments that are significantly associated with actual high mortality risk, we selected the regions characterised by higher values in all types of mortality-related vulnerability environments as high heat-wave-related mortality risk areas in the study area.

(2) Application of artificial societies

We used a model artificial society to simulate the spatial distribution of all sensitive populations. This simulation satisfied the following requirements: 1) the data feature of artificial societies is consistent with the characteristics of real populations and 2) the relationships of the artificial society are consistent with the relationships of real society.

Shanghai census data from 2010 served as the data source for this simulation. Because large-scale censuses are only conducted once per decade in China, an accurate representation of China's current population distribution was obtained for the next decade.

The artificial society is constructed based on three key algorithms.

(1) Family structure generation algorithm: In reconstructing a reasonable family structure, this article only considers family structures involving three or fewer generations because according to the China Statistics Bureau 2011 (Sumita, 2011), the three-generation family structure accounted for > 90% of the total households in China. Fig. s1 shows the process of family structure modelling based on family size.
(2) Population attribute matching: The corresponding population attribute values, including sex and age, can be assigned to individuals according to their family role. The assignment process is shown in Fig. 3b. In this process, we included three adjustable variables in the model (AHW, the age difference between husband and wife; AFC, the age difference between the mother and the eldest son; and ACC, the age difference between brothers and sisters). By adjusting for these three variables, the simulation results are consistent with real census data.
(3) Spatial mapping of the artificial society: As the final step, we attempt to provide the spatial extent regarding where the sensitive populations are located along every street. This part of the algorithm is divided into three steps according to the process order: 1) Built-up areas along each street were extracted using supervised classification based on Landsat 8 data, with an image acquisition time of 28 August 2013, which is the most recent data relevant to the 2010 census with high visibility and minimal atmospheric interference; 2) Family populations for each street were distributed in the built-up areas via a spatial calculation; and 3) The spatial distribution of sensitive populations (people under ten and over sixty years old) along each street were selected by family scale.

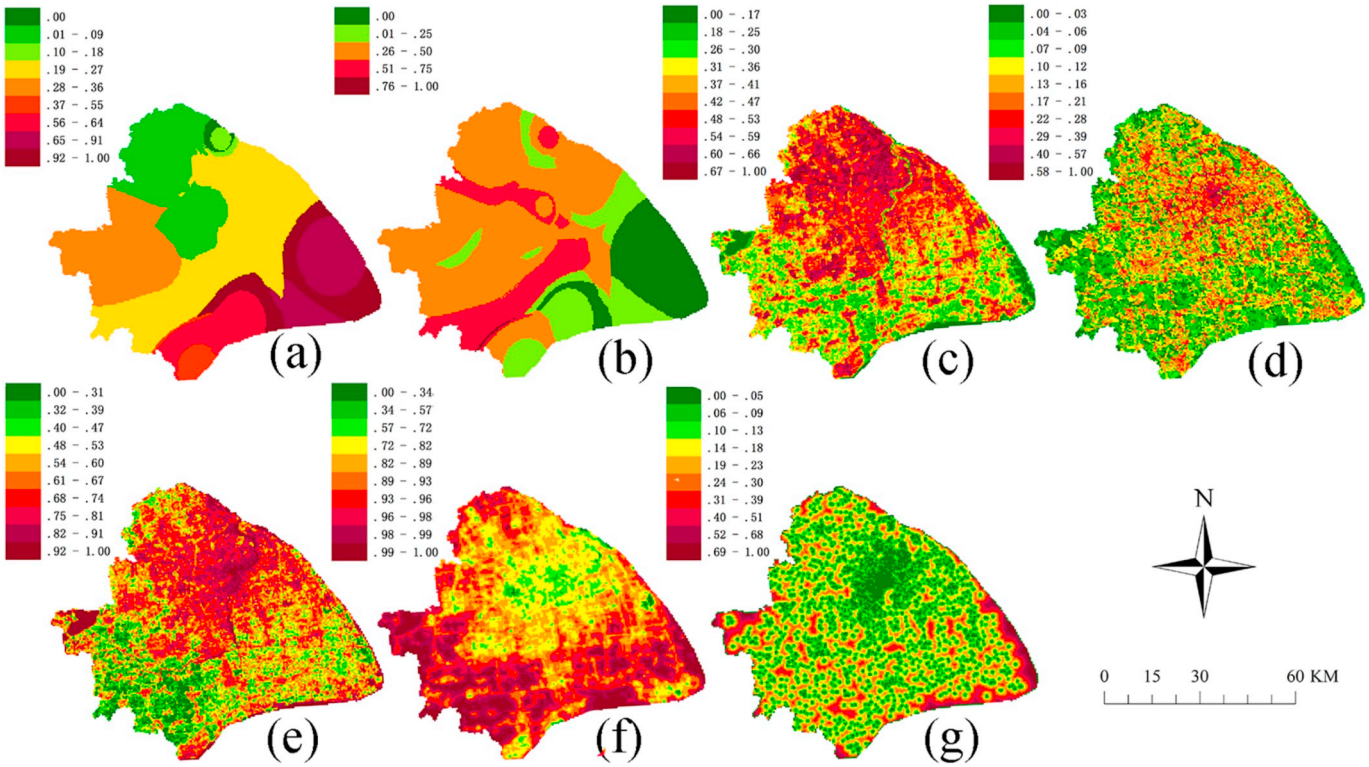

Fig. 3. (a) Spatial distribution of the HWD value; (b) spatial distribution of the HWF value; (c) spatial distribution of the HWI value; (d) spatial pattern of the density of roads; (e) spatial distribution of the vegetation coverage; (f) spatial pattern of the night-time light value; (g) spatial pattern of the availability of medical resources. The means of each indicator value are the same as in Table 1. All results were processed using the same grid size (500 m × 500 m) after standardisation.

5. Results

5.1. Spatial variation patterns of HVI components

In general, the inconsistent numerical differences among each HVI component are shown in Table 1, and the different patterns of each index are evident as shown in Fig. 3. Higher vulnerability was represented by higher evaluation scores. Significant differences were observed between each index; thus, these indices can describe the complexities of the urban system from different aspects.

Specifically, two trends were observed for every index in the spatial distribution.

a) Spatial trend from the coast to inland area. The special atmospheric environment from coastal to inland areas varies according to the influence of sea surface temperature; therefore, the coastal area's thermal environment is consistently higher in summer. Thus, HWD and HWF vary between coastal and inland areas (in coastal areas, the value of HWD is higher but the value of HWF is lower compared with that of inland areas). This result is consistent with Oliver et al.'s research (Oliver et al., 2017).
b) Spatial trends from the downtown area to the suburbs. Social and economic activities are concentrated in downtown areas, which represents an influence of urbanisation. Moreover, the effects of this phenomenon present two different aspects. First, concentrated human activity results in lower vegetation coverage, higher road density and higher level of HWI in downtown areas. Consequently, the value of these indices is higher in downtown areas. Second, under intense social economic activity, the availability of social resources is higher and socio-economic conditions are better in city centres than in suburban areas. As a result, the heat wave adaptability of downtown areas is better than that of suburban areas, which is represented in the patterns of NTL value (Fig. 3f) and medical resource availability (Fig. 3g).

In general, these indices could be integrated for these similar spatial

Table 1
Summary of assessment factor statistics for urban and suburban data (these data were collected separately) after data normalisation from 0 to 1. Because higher vulnerability is represented by higher evaluation scores, the mean values of each index are not the same: 1) higher values of HWD, HWF, HWI and Density of Roads represent longer duration, higher frequency, higher LST and higher road density, respectively. 2) higher values of Vegetation Coverage, Availability of Medical Resources and NTL represent lower coverage rate, lower availability and lower NTL values, respectively. Lower adaptability implies higher heat wave vulnerability.

Characteristic	Total	City centre	Suburbs
	(22,116 grids)	(1162 grids)	(20,954 grids)
Mean (SD) HWD	0.4224 (0.3031)	0.2001 (0.0890)	0.2001 (0.0890)
Mean (SD) HWF	0.4152 (0.2310)	0.5436 (0.1129)	0.4080 (0.2338)
Mean (SD) HWI	0.4164 (0.1371)	0.5426 (0.0817)	0.4094 (0.1362)
Mean (SD) density of roads	0.1104 (0.0893)	0.2273 (0.1451)	0.1039 (0.0803)
Mean (SD) vegetation coverage	0.6034 (0.1731)	0.7913 (0.0864)	0.5929 (0.0965)
Mean (SD) availability of medical resources	0.1505 (0.1173)	0.0560 (0.0412)	0.1557 (0.11179)
Mean (SD) NTL	0.6914 (0.1007)	0.5535 (0.0720)	0.7991 (0.0978)

Table 2
Results of the factor analysis based on varimax rotation.

Characteristic	Factor 1	Factor 2
	Exposure and sensitivity (E&S)	Lacking adaptation (LAD)
HWD	0.280	−0.017
HWF	0.153	−0.532
HWI	0.563	−0.321
Density of roads	0.55	−0.069
Vegetation coverage	0.575	0.002
Availability of medical resources	−0.319	0.432
NTL	−0.84	0.545

trends to comprehensively describe an urban environment. If all index types are integrated by using weighted sums, the method of weight definition would affect the study results and the recommendations. Therefore, we elected to integrate methods based on spatial trends from these indices.

5.2. Factor analysis

To explore the relationship between urban vulnerability environments and human health under heat wave conditions, we used the varimax rotation based on related research (Chuang and Gober, 2015) to comprehensively characterise the urban environment based on the spatial characteristics of each index.

As shown in Table 2, these indices are classified as two integrated components in an attempt to describe urban vulnerability environment factors. Moreover, according to the weight score for each index, we categorised these factors as follows: Exposure and Sensitivity (E&S) and Lacking Adaptation (LAD). Then, the spatial pattern of each factor was obtained by totalling all indices after multiplying by each weight. The spatial results are shown in Fig. 4. The numerical results show that E&S and LAD explained 30.79% and 35.57% of the variance, respectively. Together, they explained 66.36% of the overall variance.

Areas with higher values for E&S are considered to be areas with high disaster exposure or susceptibility to high temperature. As shown in Fig. 4, the E&S map has a regular distribution of values, with high values primarily distributed in the downtown and coastal areas in the east. Areas with higher values for LAD are considered to be areas with low socio-economic capacity or poor socio-economic resources. In particular, the socio-economic level in the northern part of Shanghai is evidently higher than that in other areas. Because downtown area is distributed in the north, and the values for LAD in the southern suburbs (especially the southeast coastal area), where the source of social and economic resources are limited, are the highest.

In general, the study area is divided into two factor types as shown in Fig. 4. In brief, high E&S values represent those areas characterised by high exposure and sensitivity but strong adaptability to heat waves, whereas high LAD values signify areas with low exposure and sensitivity but weak adaptability to heat waves. The downtown area is characterised by high E&S values and low LAD values because despite the concentration of human activities contributing to high urban temperatures, heat wave disaster adaptability is also enhanced by the improvement in socio-economic conditions. With regards to the health of urban residents, it is important to determine which factor is the dominant vulnerability factor for actual mortality.

5.3. Health impact analysis results

Of the 5702 grids in the Pudong area with corresponding factor values, there are 654 grids in which the number of deaths occurred in the context of a heat wave disaster. These grids are divided into two categories according to the median number of heat-wave mortalities. The results of comparing the net moderate and high mortality against the zeromortality net by using the MLR model are shown in Table 3.

The results reveal that the E&S factor is a significant predictor of the net moderate heat-wave-related mortality ratio ($p < 0.05$) [OR = 1.210; 95% CI: 1.134, and 1.428 for a 1-unit increase in the E&S factor score]. The OR value for the net high heat-wave-related mortality ratio is lower than that of the net moderate heat-wave-related mortality ratio. The LAD factor is a better predictor of the net with high heat-wave-related mortality ratio ($p < 0.05$) [OR = 1.548; 95% CI: 1.209, and 1.626 for a 1-unit increase in the LAD factor score]. However, the predictive value of the LAD factor for the net moderate heat-wave-related mortality ratio is lower (OR = 1.003). The results show that the impact of the E&S factor on residents' health does not increase with an

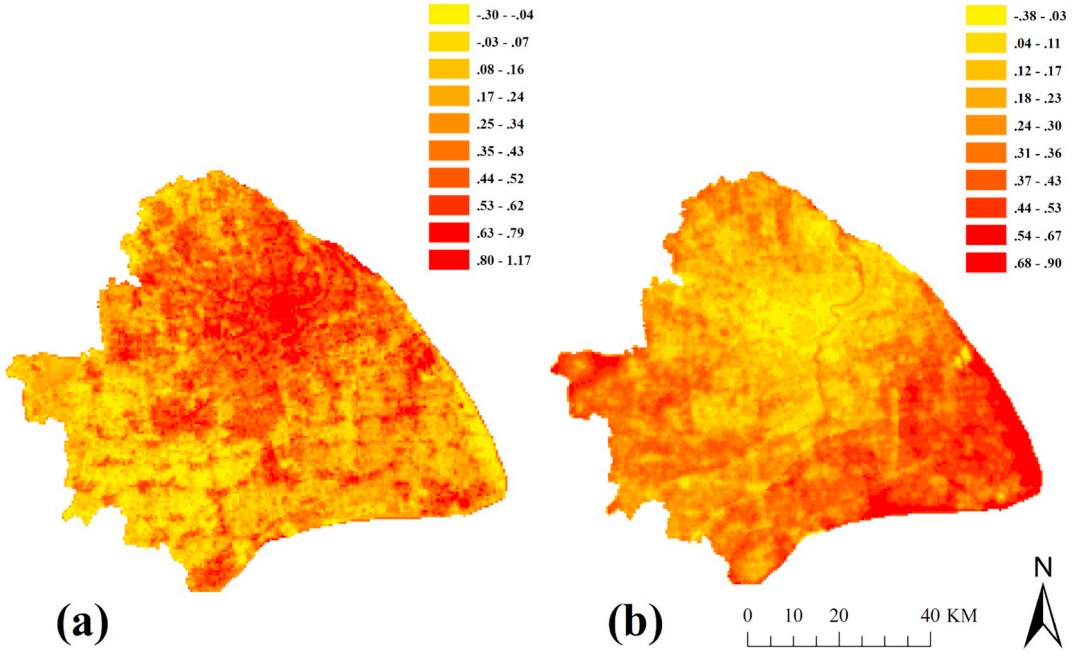

Fig. 4. Spatial pattern of the E&S factor (a) and LAD factor (b); higher vulnerability is represented by higher evaluation scores for both the E&S factor and LAD factor.

Table 3
ORs and 95% CIs for the association between a 1-unit increase in each factor and net moderate and high heat-wave-related mortality ratios based on the MLR.

Predictor	OR (95% CI)	*p*-Value
Net moderate heat-wave-related mortality ratio		
E&S factor	1.210 (1.134, 1.428)	0.032
LAD factor	1.003 (0.997, 1.007)	0.012
Net high heat-wave-related mortality ratio		
E&S factor	1.019 (1.002, 1.101)	0.037
LAD Factor	1.548 (1.209, 1.626)	0.002

increase in mortality. In other words, when the E&S factor value exceeds a certain threshold, the impact on the residents' health will not increase. In contrast, when the social resources in the surrounding areas are limited and the social connections are relatively weak, the impact of heat waves on the residents' health will be more profound.

In summary, the level of E&S effects on the lower limit of heat wave health impact and the LAD level effects on the upper limit of the heat wave impact on human health in the study area. Moreover, the E&S and LAD both influence the impact of heat waves on human health.

5.4. Mapping heat-wave-related mortality risk

The last part of the study maps the heat-wave-related mortality risk within the study area. First, we determined the heat-wave-related mortality risk area based on the values from two conditions: 1) greater than average E&S and LAD factors; or 2) > 95% values for E&S or LAD factors (because E&S and LAD are both mortality-related factors based on the results from the health impact analysis). Second, the number of sensitive populations, including individuals who are older than 60 or < 10 years old, is identified in the study area based on an artificial society as shown in Fig. s2. Moreover, we calculated the total number of sensitive populations in each district to verify the accuracy of the data and compared this number with the value from actual census data. Comparison of the results reveals that the two sets of data are equivalent. Finally, to combine the heat-wave-related mortality risk area with the sensitive populations, we extracted the spatial distribution of all grids with high mortality risk and identified the number of sensitive residents in these grids.

A heat-wave-related mortality risk distribution map was developed as shown in Fig. 5. Two trends are shown in this map: 1) The number of grids in suburban areas is significantly higher than in the city centre, indicating that heat wave vulnerability is higher in the suburbs than in the city centre, which is consistent with the results reported in relevant studies (Chen et al., 2016); and 2) Although the number of high-vulnerability risk grids in the city centre is small, the large size of the sensitive population indicates the importance of considering these areas when planning medical resources to manage heat wave disasters in the future.

6. Discussion

In this study, we comprehensively describe heat wave vulnerability environments using multi-source geographic data and evaluate how accurately these vulnerability environments reflect actual mortality at urban area. Comprehensive vulnerability environments can be divided into two opposing types using varimax rotation. Generally, the development of these two opposing trends is a result of urbanisation, wherein many residents migrate to downtown areas. Concentrated populations lead to increased anthropologic heat, which alters the heat wave exposure and sensitivity patterns. At the same time, urbanisation also promotes the social economy of downtown areas, which can enhance heat wave adaptability in these areas. These opposing trends are therefore represented in the same area as shown in Fig. 4a and b.

Furthermore, we try to use the MLR model to evaluate the location and type of urban environment that is at risk of heat-related mortality caused by one of these two vulnerability environments. The results showed that, in the study area, the E&S factor impacts the lower limit of the heat wave's effect on resident health and the LAD factor impacts the upper limit of the heat wave's effect on human health. In addition, the impacts of the E&S and LAD factors on human health will likely change in the future as a result of urbanisation. Specifically, the LAD factor will have more profound and lasting impacts because of the distinct LAD factor effects on the net with high heat-wave-related mortality ratio. The effects of E&S factor, however, will be gradually weaken because the effects on resident health do not increase when the E&S factor value exceeds a certain threshold.

Finally, this study maps heat-wave-related mortality risk based on a combination of research on vulnerability environments and artificial societies. The map reveals that the sensitive populations distributed in suburban area, especially those in suburbs that are near the downtown area and coast, experience high heat-wave-related mortality risk. On the one hand, suburbs close to the downtown include larger-sized sensitive populations, yet with generally lower social and economic conditions. On the other hand, suburbs near coastal experience a higher level of high-temperature exposure and present relatively lower social economic condition. In other suburbs, the risk levels varied depending on the influence of different socio-economic conditions and temperature conditions. Compared with the suburbs, few high-risk grids are observed within the city centre despite this area accumulating a large number of sensitive populations. In summary, it is important to consider these two types of areas when planning socioeconomic resources responses to heat wave disaster.

In the near future, young people will relocate to city centres with the expansion of urbanisation. More importantly, a high proportion of the ageing and early childhood populations will become “empty nests” in the suburbs (Chen et al., 2016). The social isolation of these empty nest populations is more severe when coupled with the limited availability of social and economic resources in suburban areas, which will increase the overall level of high-temperature vulnerability of future suburban populations. The results presented in this study reveal that adaptability has a clear effect on the risk of heat-wave-associated mortality. Therefore, the allocation of social resources and sensitive populations must be considered in an effort to address climate change in suburban areas.

The innovations of this study are reflected in the following two aspects.

a) The index assessment method. Both satellite data and meteorological observation data were used to evaluate the heat wave exposure pattern. Additionally, NTL and POI data were used to evaluate socio-economic activities. Lastly, the distribution of sensitive populations within the city was depicted using artificial societies. To the best of our knowledge, this is the first vulnerability assessment within an urban interior that has overcome statistical scale limitations.
b) The map of heat-wave-related mortality risk in Shanghai provides direct evidence for several findings. 1) Due to a strong adaptability to heat waves, the areas with high heat wave vulnerability in the downtown area are relatively small. Each high-risk grid, however, is distributed across a large number of sensitive populations, indicating that medical resource planning still requires attention in this area. 2) Heat wave vulnerability areas are not confined to densely populated regions. Sensitive populations living in the suburbs are also vulnerable to heat waves. Especially in estuarine cities, such as Shanghai, where temperature changes are complex, a large number of high-risk grids were distributed in the suburbs. These conclusions are consistent with the results of previous heat-wave-related mortality studies conducted in China, which found that mortality rates were relatively stable in the central parts of cities

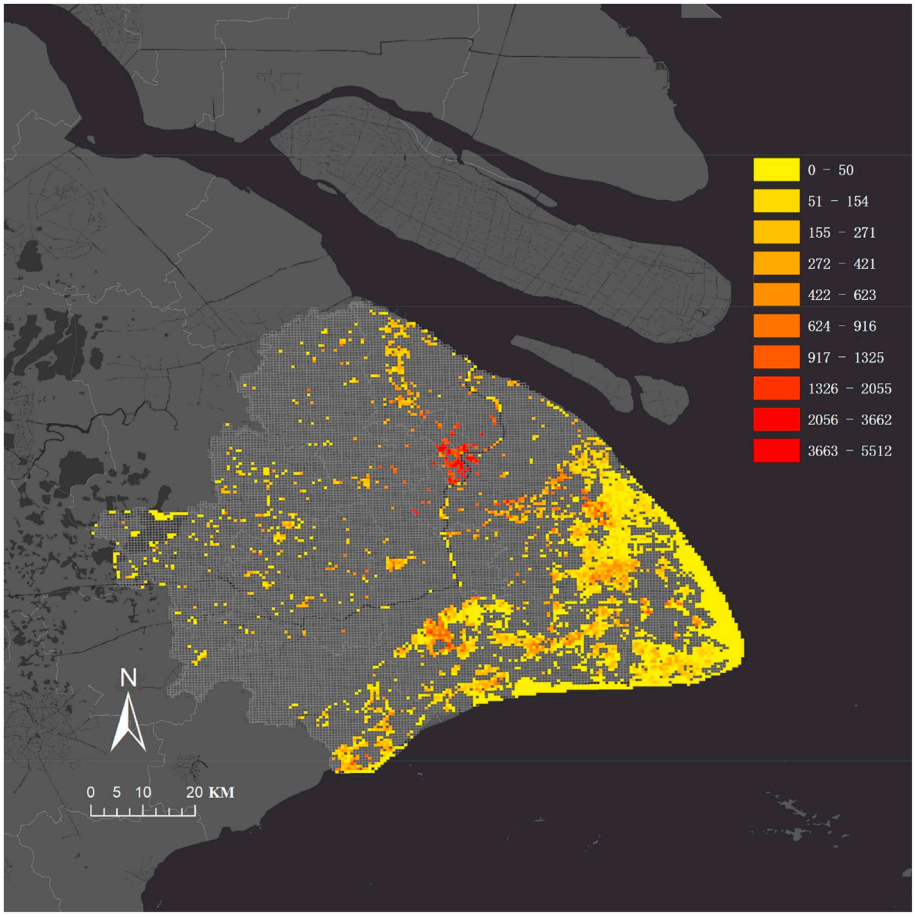

Fig. 5. Mortality risk distribution map for heat wave disasters. Areas with HVI values > 3.2 are identified as high-risk areas. The number of sensitive populations in these areas is shown based on an artificial society.

during heat waves but noticeably higher in the suburbs (Chen et al., 2016; Gong et al., 2012). Furthermore, studies from other countries also support this conclusion. For example, in the United States, heat-related mortality was significantly higher in the suburbs during heat waves (Madrigano et al., 2015b); and in France, temperatures in the suburbs were unstable and medical resources were limited during a heat wave disaster (Todd and Valleron, 2015). In summary, quantitative and innovative methods were implemented in this study to support these relevant conclusions.

Some of the study's limitations should also be recognised. First, certain variables associated with health concerns that may affect heat wave vulnerability, such as disabilities and past medical history, were not addressed in this study. With improvements in statistical collection methods, these additional relevant variables should be included in future artificial society simulations. Second, recent research determined that ozone is also an important indicator that affects heat-related mortality (Anderson and Bell, 2009). However, ozone data were not recorded between 2010 and 2015 for the study area and were not included here. Third, our analysis was limited by a lack of index data at the long-term scale. Therefore, we only considered the recent situation. However, the relationship between the impacts of E&S and LAD on human health is dynamic in the urbanisation process. To better understand the location and type of urban environment that is at risk of heat-related mortality in the future, a comparison study must be performed for different years. Finally, we limited our analysis to urban areas and conducted our study for one city in China. The results of this study may not be applicable to regions with different climatic conditions, such as inland cities, which are less affected by ocean currents.

Despite these limitations, our research is one of a few studies in China to comprehensively describe urban environment vulnerability and study its connection with mortality within a single coastal urban area. By using multi-source spatial data to inform the different spatial aspects of urbanisation features, we were able to evaluate which types of vulnerability environments are at risk of heat-related mortality caused by the varying features of urbanisation. Furthermore, by applying an artificial society to simulate the spatial distribution of sensitive populations, we were able to visually depict those sensitive populations in Shanghai that are located in high heat-wave-related mortality risk areas during heat waves without the scale limitation of population statistics. These tools introduce a methodological system for studying the relationship between urbanisation and human health that can serve as a template for future comprehensive research at the local level. Additionally, in actual heat wave disaster prevention planning, these study results can provide a reference for preventing heat-related deaths.

In the future, we hope to use a greater range of health data to validate our measurement of heat wave vulnerability in different areas and during different time periods. This information could further highlight local differences among factors that contribute the most to vulnerability.

7. Conclusions

In this study, we used various approaches to assess heat wave vulnerability at the city level by integrating data from remote sensing, artificial society simulation and other multi-source geographic information. By using innovative assessment methods for each vulnerability index, we overcame the scale limit of statistical data.

The results of the factor analysis led to several conclusions. First, different aspects of urbanisation have different impacts on disaster vulnerability. In the present case, the exposure level and sensitivity factors are increased because the city's thermal environment and ecosystem have been altered by the increasing intensity of human activity in the process of urbanisation. However, the level of high temperature adaptability is simultaneously enhanced by the rising social and economic level of residents. Second, we explored the relationship between these two influential urbanisation aspects and heat-wave-related mortality using MLR. The results reveal that, in the study area, the E&S factor impacts the lower limit of heat-wave-related effects on residents' health and the LAD factor impacts the upper limit of the heat-wave-related effects on human health.

Finally, we used the high value of these two factors combined with the spatial distribution of sensitive populations obtained by using the artificial society algorithm to map the distribution of heat-wave-related mortality risk in Shanghai. The results reveal that the high-risk areas of heat-wave-related mortality are not limited to the city centre but also extend to the suburbs in coastal areas. Because of the ageing rural population trend, this problem should be addressed.

This study demonstrates that vulnerability assessments can be performed by mapping the vulnerability level within cities using multiple sources of data and high spatial scale factors. Additionally, valuable suggestions are presented to optimise local area studies on the effects of heat waves on human health. And also, this study can provide valuable inputs and decision-making support for planners and managers to reduce the risks under an increasing trend of urban heat wave disasters in the future.

Acknowledgements

This work was funded by National Key Research and Development Program of China (2016YFC0502706).

Appendix A. Supplementary data

Supplementary data to this article can be found online at https://doi.org/10.1016/j.envint.2019.01.057.

References

Alana, H., Peng, B., Monika, N., Philip, R., Dino, P., Graeme, T.J.E.H.P., 2008. The Effect of Heat Waves on Mental Health in a Temperate Australian City. 116. pp. 1369–1375.
Anderson, B.G., Bell, M.L., 2009. Weather-related mortality how heat, cold, and heat waves affect mortality in the United States. Epidemiology 20, 205–213.
Anderson, G.B., Oleson, K.W., Jones, B., Peng, R.D.J.C.C., 2016. Projected Trends in High-Mortality Heatwaves Under Different Scenarios of Climate, Population, and Adaptation in 82 US Communities. 146. pp. 1–16.
Andriacchi, T.P., Ogle, J.A., Galante, J.O., 1977. Walking speed as a basis for normal and abnormal gait measurements. J. Biomech. 10, 261–268.
Aubrecht, C., Ozceylan, D., 2013. Identification of heat risk patterns in the U.S. National Capital Region by integrating heat stress and related vulnerability. Environ. Int. 56, 65–77.
Basu, R., 2009. High ambient temperature and mortality: a review of epidemiologic studies from 2001 to 2008. Environ. Health 8.
Braga, A.L.F., Zanobetti, A., Schwartz, J., 2002. The effect of weather on respiratory and cardiovascular deaths in 12 US cities. Environ. Health Perspect. 110, 859–863.
Cai, J.X., Huang, B., Song, Y.M., 2017. Using multi-source geospatial big data to identify the structure of polycentric cities. Remote Sens. Environ. 202, 210–221.
Chen, K., Zhou, L., Chen, X.D., Ma, Z.W., Liu, Y., Huang, L., Bi, J., Kinney, P.L., 2016. Urbanization level and vulnerability to heat-related mortality in Jiangsu Province, China. Environ. Health Perspect. 124, 1863–1869.
Chien, L.C., Guo, Y., Zhang, K.J.S., 2016. Spatiotemporal Analysis of Heat and Heat Wave Effects on Elderly Mortality in Texas, 2006–2011. 562. pp. 845–851.
Chow, W.T.L., Salamanca, F., Georgescu, M., Mahalov, A., Milne, J.M., Ruddell, B.L., 2014. A multi-method and multi-scale approach for estimating city-wide anthropogenic heat fluxes. Atmos. Environ. 99, 64–76.
Chuang, W.C., Gober, P., 2015. Predicting hospitalization for heat-related illness at the census-tract level: accuracy of a generic heat vulnerability index in Phoenix, Arizona (USA). Environ. Health Perspect. 123, 606–612.
Coll, C., Galve, J.M., Sanchez, J.M., Caselles, V., 2010. Validation of Landsat-7/ETM+ thermal-band calibration and atmospheric correction with ground-based measurements. IEEE Trans. Geosci. Remote Sens. 48, 547–555.
Curriero, F.C., Heiner, K.S., Samet, J.M., Zeger, S.L., Strug, L., Patz, J.A., 2002. Temperature and mortality in 11 cities of the eastern United States. Am. J. Epidemiol. 155, 80–87.
Cutter, S.L., Finch, C., 2008. Temporal and spatial changes in social vulnerability to natural hazards. Proc. Natl. Acad. Sci. U. S. A. 105, 2301–2306.
Della-Marta, P.M., Luterbacher, J., von Weissenfluh, H., Xoplaki, E., Brunet, M., Wanner, H., 2007. Summer heat waves over western Europe 1880–2003, their relationship to large-scale forcings and predictability. Clim. Dyn. 29, 251–275.
Diaz, J., Carmona, R., Miron, I.J., Ortiz, C., Leon, I., Linares, C., 2015. Geographical variation in relative risks associated with heat: update of Spain's heat wave prevention plan. Environ. Int. 85, 273–283.
Díaz, J., Carmona, R., Mirón, I.J., Luna, M.Y., Linares, C.J.E.I., 2018. Time Trend in the Impact of Heat Waves on Daily Mortality in Spain for a Period of Over Thirty Years (1983–2013). 116. pp. 10–17.
Epstein, J.M., 2009. Modelling to contain pandemics. Nature 460, 687.
Fallmann, J., Forkel, R., Emeis, S., 2016. Secondary effects of urban heat island mitigation measures on air quality. Atmos. Environ. 125, 199–211.
Fouillet, A., Rey, G., Laurent, F., Pavillon, G., Bellec, S., Guihenneuc-Jouyaux, C., Clavel, J., Jougla, E., Hemon, D., 2006. Excess mortality related to the August 2003 heat wave in France. Int. Arch. Occup. Environ. Health 80, 16–24.
Fussel, H.M., 2007. Adaptation planning for climate change: concepts, assessment approaches, and key lessons. Sustain. Sci. 2, 265–275.
Giannaros, T.M., Melas, D., Daglis, I.A., Keramitsoglou, I., Kourtidis, K., 2013. Numerical study of the urban heat island over Athens (Greece) with the WRF model. Atmos. Environ. 73, 103–111.
Gong, P., Liang, S., Carlton, E.J., Jiang, Q., Wu, J., Wang, L., Remais, J.V.J.L., 2012. Urbanisation and Health in China. 379. pp. 843–852.
Hajat, S., Sheridan, S.C., Allen, M.J., Pascal, M., Laaidi, K., Yagouti, A., Bickis, U., Tobias, A., Bourque, D., Armstrong, B.G., Kosatsky, T., 2010. Heat-health warning systems: a comparison of the predictive capacity of different approaches to identifying dangerously hot days. Am. J. Public Health 100, 1137–1144.
Han, L., Zhou, W., Li, W., Qian, Y.J.S., 2018. Urbanization Strategy and Environmental Changes: An Insight With Relationship Between Population Change and Fine Particulate Pollution. 642. pp. 789–799.
Hauser, M., Orth, R., Seneviratne, S.I., 2016. Role of soil moisture versus recent climate change for the 2010 heat wave in western Russia. Geophys. Res. Lett. 43, 2819–2826.
Helbing, D., 2013. Globally networked risks and how to respond. Nature 497, 51–59.
Ho, H.C., Knudby, A., Walker, B.B., Henderson, S.B., 2017. Delineation of spatial variability in the temperature-mortality relationship on extremely hot days in greater Vancouver, Canada. Environ. Health Perspect. 125, 66–75.
Hondula, D.M., Davis, R.E., Saha, M.V., Wegner, C.R., Veazey, L.M.J.E.R., 2015. Geographic Dimensions of Heat-Related Mortality in Seven U.S. Cities. 138. pp. 439–452.
Huang, W., Kan, H.D., Kovats, S., 2010. The impact of the 2003 heat wave on mortality in Shanghai, China. Sci. Total Environ. 408, 2418–2420.
Hudson, G., Wackernagel, H.J.I.J., 2010. Mapping Temperature Using Kriging With External Drift: Theory and an Example From Scotland. 14. pp. 77–91.
IPCC, 2007. In: IPCC (2007): Climate Change the Physical Science Basis. AGU Fall Meeting.
IPCC, 2014. Climate Change 2014: Synthesis Report. Cambridge University Press, Cambridge, United Kingdom and New York.
Johnson, D.P., Stanforth, A., Lulla, V., Luber, G.J.A.G., 2012. Developing an Applied Extreme Heat Vulnerability Index Utilizing Socioeconomic and Environmental Data. 35. pp. 23–31.
Jordan, R., Birkin, M., Evans, A., 2012. Agent-Based Modelling of Residential Mobility, Housing Choice and Regeneration. Springer, Netherlands.
Keellings, D., Waylen, P.J.A.G., 2014. Increased Risk of Heat Waves in Florida: Characterizing Changes in Bivariate Heat Wave Risk Using Extreme Value Analysis. 46. pp. 90–97.
Kelly, P.M., Change, W.N.A.J.C., 2000. Theory and Practice in Assessing Vulnerability to Climate Change andFacilitating Adaptation. 47. pp. 325–352.
Krstic, N., Yuchi, W., Ho, H.C., Walker, B.B., Knudby, A.J., Henderson, S.B., 2017. The heat exposure integrated deprivation index (HEIDI): a data-driven approach to quantifying neighborhood risk during extreme hot weather. Environ. Int. 109, 42–52.
Li, F., Chen, W., Zeng, Y., Zhao, Q., Wu, B.J.R.S., 2014. Improving Estimates of Grassland Fractional Vegetation Cover Based on a Pixel Dichotomy Model: A Case Study in Inner Mongolia, China. 6. pp. 4705–4722.
Liu, H.X., Li, F., Li, J.Y., Zhang, Y.Y., 2017. The relationships between urban parks, residents' physical activity, and mental health benefits: a case study from Beijing, China. J. Environ. Manag. 190, 223–230.
Madrigano, J., Ito, K., Johnson, S., Kinney, P.L., Matte, T., 2015a. A case-only study of vulnerability to heat wave-related mortality in New York City (2000−2011). Environ. Health Perspect. 123, 672–678.
Madrigano, J., Jack, D., Anderson, G.B., Bell, M.L., Kinney, P.L., 2015b. Temperature, ozone, and mortality in urban and non-urban counties in the northeastern United States. Environ. Health 14.
Marsha, A., Sain, S.R., Heaton, M.J., Monaghan, A.J., Wilhelmi, O.V.J.C.C., 2018. Influences of Climatic and Population Changes on Heat-Related Mortality in Houston, Texas, USA. pp. 1–15.
Mazdiyasni, O., AghaKouchak, A., Davis, S.J., Madadgar, S., Mehran, A., Ragno, E., Sadegh, M., Sengupta, A., Ghosh, S., Dhanya, C.T., Niknejad, M., 2017. Increasing probability of mortality during Indian heat waves. Sci. Adv. 3.
Oliver, E.C.J., Benthuysen, J.A., Bindoff, N.L., Hobday, A.J., Holbrook, N.J., Mundy, C.N., Perkins-Kirkpatrick, S.E., 2017. The unprecedented 2015/16 Tasman Sea marine heatwave. Nat. Commun. 8.

Puliafito, S.E., Allende, D., Pinto, S., Castesana, P.J.A.E., 2015. High resoluTion Inventory of GHG Emissions of the Road Transport Sector in Argentina. 101. pp. 303–311.
Reid, C.E., O'Neill, M.S., Gronlund, C.J., Brines, S.J., Brown, D.G., Diez-Roux, A.V., Schwartz, J., 2009. Mapping community determinants of heat vulnerability. Environ. Health Perspect. 117, 1730–1736.
Semenza, J.C., Rubin, C.H., Falter, K.H., Selanikio, J.D., Flanders, W.D., Howe, H.L., Wilhelm, J.L., 1996. Heat-related deaths during the July 1995 heat wave in Chicago. N. Engl. J. Med. 335, 84–90.
Sumita, M.J.C.P.T., 2011. Communiqué of the National Bureau of Statistics of People's Republic of China on Major Figures of the 2010 Population Census (No. 1). 6. pp. 19–23.
Sun, R.H., Wang, Y.N., Chen, L.D., 2018. A distributed model for quantifying temporal-spatial patterns of anthropogenic heat based on energy consumption. J. Clean. Prod. 170, 601–609.
Tan, J.G., Zheng, Y.F., Song, G.X., Kalkstein, L.S., Kalkstein, A.J., Tang, X., 2007. Heat wave impacts on mortality in Shanghai, 1998 and 2003. Int. J. Biometeorol. 51, 193–200.
Todd, N., Valleron, A.J., 2015. Space-time covariation of mortality with temperature: a systematic study of deaths in France, 1968-2009. Environ. Health Perspect. 123, 659–664.
Turner, L.R., Barnett, A.G., Connell, D., Tong, S.L., 2012. Ambient temperature and cardiorespiratory morbidity a systematic review and meta-analysis. Epidemiology 23, 594–606.
Uejio, C.K., Wilhelmi, O.V., Golden, J.S., Mills, D.M., Gulino, S.P., Samenow, J.P., 2011. Intra-urban societal vulnerability to extreme heat: the role of heat exposure and the built environment, socioeconomics, and neighborhood stability. Health Place 17, 498–507.
Westermann, S., Langer, M., Boike, J.J.R.S., 2011. Spatial and Temporal Variations of Summer Surface Temperatures of High-Arctic Tundra on Svalbard — Implications for MODIS LST Based Permafrost Monitoring. 115. pp. 908–922.
Wood, J.M., Tataryn, D.J., Gorsuch, R.L.J.P.M., 1996. Effects of Under- and Overextraction on Principal Axis Factor Analysis With Varimax Rotation. 1. pp. 354–365.
Wu, B.M., Birkin, M.H., 2012. Agent-Based Extensions to a Spatial Microsimulation Model of Demographic Change. Springer, Netherlands.
Zhang, Q.L., Seto, K.C., 2011. Mapping urbanization dynamics at regional and global scales using multi-temporal DMSP/OLS nighttime light data. Remote Sens. Environ. 115, 2320–2329.
Zhen, F., Cao, Y., Qin, X., Wang, B.J.C., 2017. Delineation of an Urban Agglomeration Boundary Based on Sina Weibo Microblog 'Check-in' Data: A Case Study of the Yangtze River Delta. 60. pp. 180–191.
Zheng, B., Myint, S.W., Fan, C.J.L., Planning, U., 2014. Spatial Configuration of Anthropogenic Land Cover Impacts on Urban Warming. 130. pp. 104–111.
Zheng, Q.M., Weng, Q.H., Huang, L.Y., Wang, K., Deng, J.S., Jiang, R.W., Ye, Z.R., 2018. Gan, M.Y. A new source of multi-spectral high spatial resolution night-time light imagery-JL1-3B. Remote Sens. Environ. 215, 300–312.